AN EXPERIMENTAL INVESTIGATION INTO DAMAGE MODES AND SCALE EFFECTS IN CFRP OPEN HOLE TENSION COUPONS

A.C. Orifici*, I. Herszberg+

*** School of Aerospace, Mechanical and Manufacturing Engineering**
RMIT University, GPO Box 2476, Melbourne, Victoria 3001, Australia
corresponding author: adrian.orifici@rmit.edu.au

+ Cooperative Research Centre for Advanced Composite Structures (CRC-ACS) Ltd
506 Lorimer St, Fishermans Bend, Victoria 3207, Australia

Keywords: *Composite materials, experimental testing, damage modes, notch effects, scale effects*

Abstract

An experimental investigation was conducted to study the effect of notch size and length scale on the damage of carbon fibre-reinforced composite specimens. Open hole tension specimens in a range of configurations were tested quasi-statically to ultimate failure. The load response, damage modes and strain field development were experimentally recorded. The results demonstrated that changing the ply thickness and specimen dimensions markedly affected the damage modes and specimen behaviour. This output provides key insights into the nature of composite behaviour, and is also critical for the development and validation of analysis methodologies capturing damage initiation and progression.

1 Introduction

Fibre-reinforced polymer (FRP) composites are finding increasing application in aerospace, marine and many other industries due to the advantages they provide in performance, structural efficiency and cost. However, despite years of extensive research around the world, an accurate, robust and validated methodology for predicting the behaviour of composite structures including the effects of damage has not yet been fully adopted by the technical community as a design or material certification and qualification tool. One aspect that remains critical for composite materials is the issue of scale effects, where damage initiation and progression can be significantly influenced by the relative size of the specimen, any notches or structural details, and the thickness of the composite plies.

In this work, an experimental investigation was conducted into the damage modes, notched performance and scale effects of carbon fibre reinforced polymer (CFRP) composite coupons. A range of open hole (OH) coupons were tested in quasi-static tension loading until ultimate failure. Different configurations were investigated, where the hole size was used to scale the specimen dimension, and two different stacking sequences were used to investigate the effect of ply thickness. The goal of the study was to experimentally characterise the damage modes and scale effects, and investigate the relationship between damage progression and the surface strain field. This output is critical for the development and validation of analysis methodologies capturing damage initiation and progression, such as those described in a companion paper [1].

2 Specimen Design and Test Procedure

A summary of the OH configurations investigated is given in Fig. 1. The coupons were manufactured from AS4/3501-6 carbon/epoxy uni-directional prepreg, with nominal ply thickness t_{ply} = 0.13 mm. Coupons were tested in un-notched (OH-00), 0.5" hole (OH-05) and 1.0" hole (OH-10) configurations. For the coupons with holes, the in-plane dimensions were scaled with the hole diameter. Two different quasi-isotropic laminates were tested, which both used the same number and orientation of plies in different laminate sequences: a "single-ply" dispersed laminate with ply angle changes every ply; and, a "four-ply" laminate with ply angle changes every four plies. The holes were manufactured with diamond-tip drill bits and sacrificial plates on the front and back surface to prevent delamination. There were 6 coupons in each configuration, for a total of 36 coupons.

Specimens were loaded in tension quasi-statically until ultimate failure. All tests were conducted at the Defence Science and Technology Organisation (DSTO), Melbourne. Eight of the tests were conducted on a 100 kN mechanical test machine, four tests were conducted on a 250 kN MTS hydraulic test machine, and the remainder were conducted on a 250 kN Instron hydraulic test machine. No difference in specimen performance was noted between test machines.

Strain gauges (SGs) were applied in the far-field region and adjacent to the hole on one side of the specimen, as shown in Fig. 2. Both SGs were in the loading direction, or 0° direction as shown in Fig. 1. On the other side of the specimen an optical full-field strain measurement system was applied, which tracked the movement during the test of dots painted onto the specimen surface. The dots were painted with white water-based paint using a screen-printing process, where a circular dot pattern was designed to use a dot size of 1 mm and average dot spacing (centre to centre) of 2 mm. The processing of the test images was conducted using the REMDIS2D software package, from the Computational Multiphysics Systems Laboratory of the U.S. Naval Research Laboratory [2-5].

From each test, a range of output was generated. The ultimate load for each specimen corresponded to the maximum load in the test, and was used to calculate the maximum stress, σ_{max}, using the nominal undeformed cross-sectional area. For failure initiation, two techniques were used that were based on the strain history at the hole gauge (or far-field gauge for the un-notched specimens). One technique was based on observing 5% non-linearity (5% NL), taken as a deviation of 5% from a linear fit to the initial load-strain results. At this load, the strain, ε_{NL}, was recorded. This was a robust method that could be applied to all specimens. However, as the 5% deviation from non-linearity was thought not to capture the exact initiation point, particularly for mild non-linearity, a second technique was used. In the second technique, any noticeable deviation in the strain field was used, as identified in the strain-time data. In absence of this, the point at which the load-strain data began to show non-linearity was taken. These two points are illustrated in Fig. 3. The strain and stress corresponding to either of these observations was recorded as ε_{obs} and σ_{obs}.

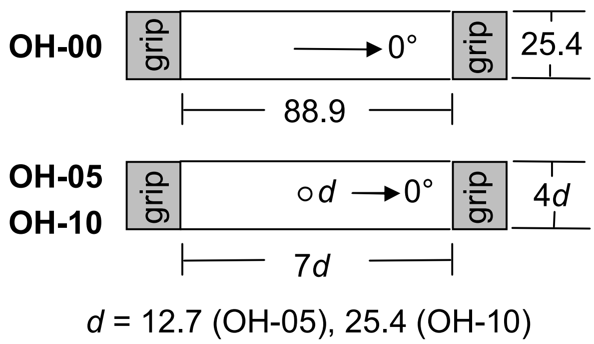

Number of specimens

OH-	00	05	10
$[+45, 0, -45]_{4S}$	6	6	6
$[+45_4, 0_4, -45_4]_S$	6	6	6

Fig. 1. Specimen details, dimensions in mm

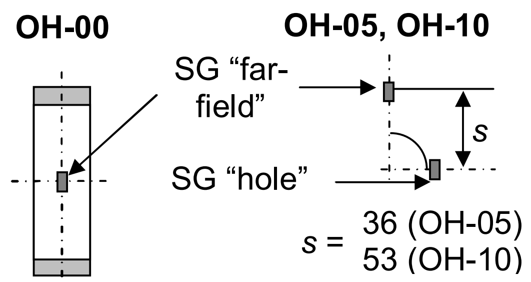

Fig. 2. SG (centre) locations, dimensions in mm

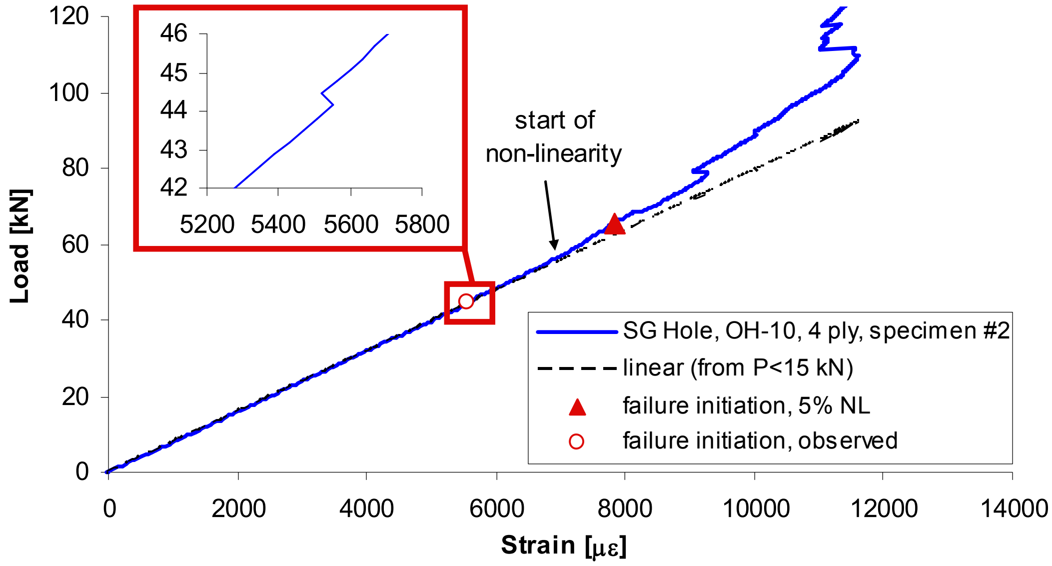

Fig. 3. Example of failure initiation definition using strain gauge history

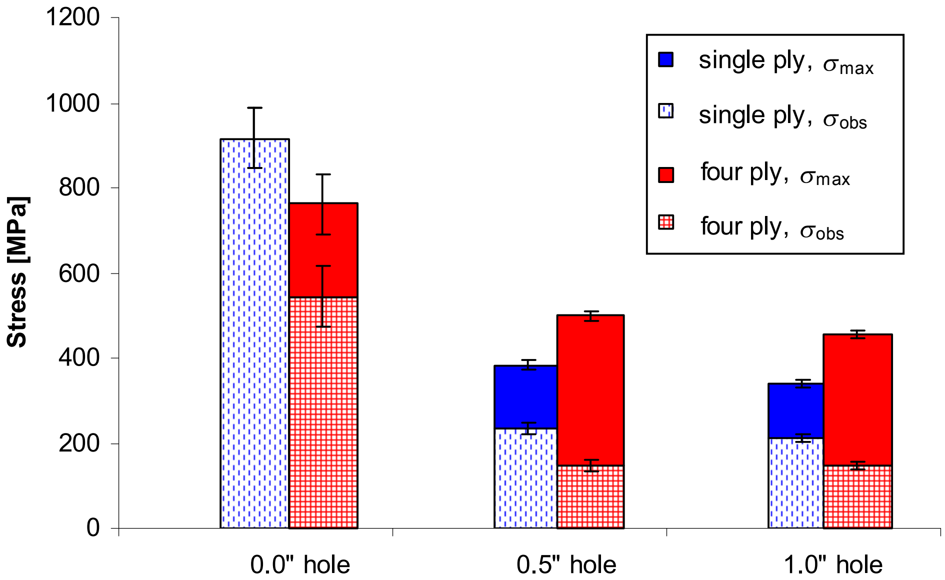

Fig. 4. Average stress results for damage initiation and ultimate load.

Table 1. Average damage initiation strain results and standard deviation (STDEV)

	single ply *0.0" hole*	***four ply*** *0.0" hole*	***single ply*** *0.5" hole*	***four ply*** *0.5" hole*	***single ply*** *1.0" hole*	***four ply*** *1.0" hole*
ε_{NL} [με]	14,672	12,563	11,643	7,806	12,859	7,079
STDEV	7%	7%	8%	8%	3%	12%
ε_{obs} [με]	14,672	9,014	6,902	4,412	8,018	5,658
STDEV	7%	9%	4%	13%	5%	6%

Specimen		Dominant failure mode		
		0.0” hole	0.5” hole	1.0” hole
single ply	$[+45, 0, -45]_{4S}$	grip	tension	tension
four ply	$[+45_4, 0_4, -45_4]_S$	grip	delamination	delamination

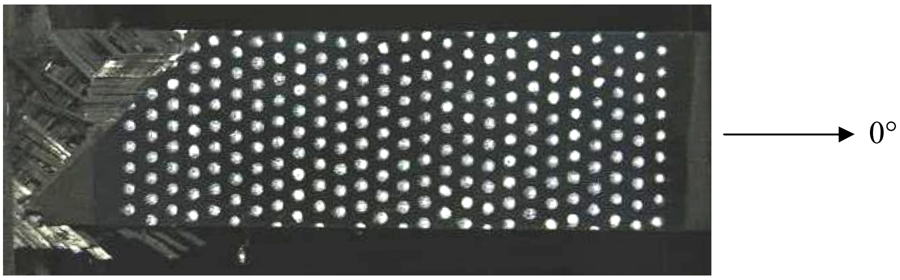

Grip failure (shown for single ply, 0.0” hole)

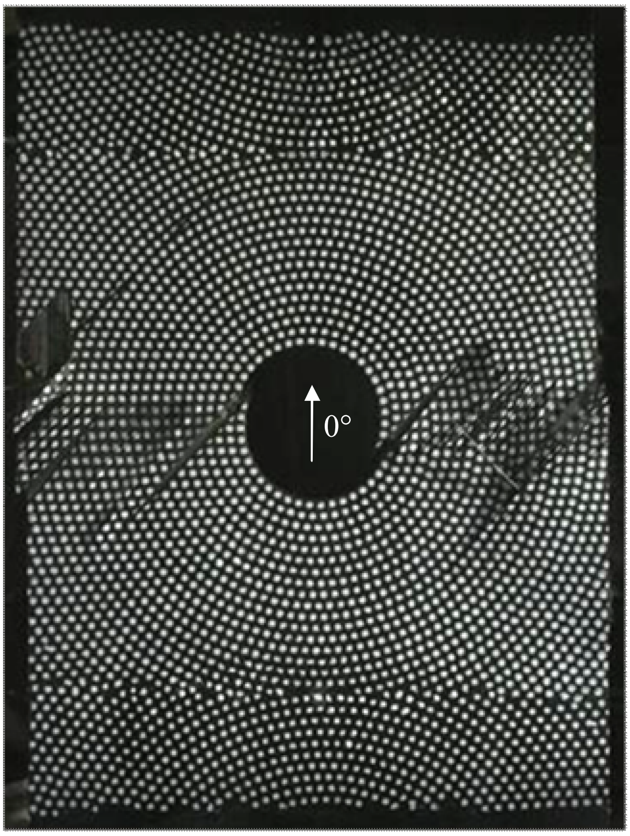

Net tension failure
(shown for single ply, 1.0” hole)

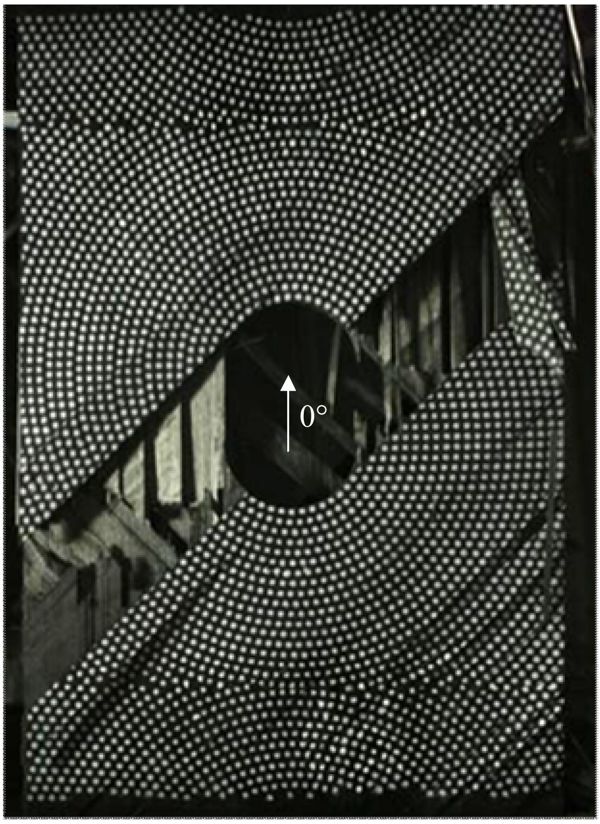

Delamination failure
(shown for four ply, 1.0” hole)

Fig. 5. Failure modes of specimens after ultimate load

3 Experimental Results

The results of the tests are summarised in Fig. 4, Table 1 and Fig. 5, where Fig. 4 gives the average stress results for damage initiation and progression, Table 1 summarises the average strain results for damage initiation using the two techniques, and Fig. 5 summarises the damage modes seen in the tests at ultimate load.

3.1 Un-notched (OH-00) Specimens

For the un-notched specimens, an ultimate strength of 916 MPa and 768 MPa was seen for the single ply and four ply specimens. With regards to strain, the values of 5% non-linearity all correspond to the ultimate failure of the specimen. As such, the ε_{NL} values of 14,672 με and 12,563 με correspond to the ultimate strain of the un-notched specimens. Both of these results demonstrate that the ultimate strength and strain of the four ply specimens was around 85% of the single ply specimens. The failure mode of both un-notched specimens was predominantly grip failure, which was expected as tabs were not used.

With regards to damage initiation, the single ply specimens did not show any non-linearity in the strain results prior to failure. In fact, although a slight amount of non-linearity was seen, it was not significant enough to be accurately distinguished. So, the ε_{obs} values reported in Table 1 correspond to the ultimate load. On the other hand, for the four ply specimens there was noticeable non-linearity in the strain results prior to ultimate load. This occurred on average at 72% of the ultimate strain of the four ply specimens. Despite this identifiable non-linearity, the strain results did not deviate significantly from linearity, and the 5% NL values for the four ply tests all correspond to the ultimate load.

3.2 0.5” hole (OH-05) Specimens

For the 0.5” hole specimens, the initiation of damage as indicated by the observed non-linearity ε_{obs} occurred at 6,902 με and 4,412 με for the single ply and four ply specimens respectively. This corresponds to an initiation of damage at around 48% of the observed damage initiation of the un-notched specimens. This indicates that whilst the strength of the four ply laminate was lower, the introduction of the notch triggered damage initiation in a similar manner for both laminates.

With regards to the damage mode and ultimate failure, the two laminates displayed quite different behaviour for the notched specimens. For the single ply specimens with the 0.5” hole, the load was seen to increase monotonically, and there was no change in character of either the load or strain results up until ultimate load. As mentioned, there was non-linearity in the hole gauge strain data. This indicates that prior to ultimate failure, only minor damage was present, which is likely to have been matrix cracking with possibly slight delamination. The failure mode of these specimens following ultimate failure was seen to be predominantly tension failure, as shown in Fig. 5, where fibre fracture spread from the hole edge perpendicular to the applied load. This involved a small amount of delamination and ply splitting, such that although in general the cracking migrated perpendicular to the load, the fracture appeared jagged on the surface of the specimen as shown in Fig. 5.

In contrast, for the 0.5” four ply specimens, all specimens except one showed some load drop before the ultimate load was reached. Additionally, the hole gauge and far-field gauges both demonstrated step changes prior to ultimate load, where typically three to four changes were seen for each test. These step changes in load and strain all occurred after the onset of non-linearity. As such, it is likely that the matrix cracks at the hole edge migrated into the interlaminate interfaces, and the step changes in load and strain correspond to instances of delamination growth. The failure mode of all of the 0.5” four ply specimens showed extensive delamination, where the region affected by delamination extended from the hole to the grips on either side of the specimen. This demonstrates a clear change in failure mode for the two laminates, where the 0.5” single ply laminates failed predominately in tension failure, whilst the 0.5” four ply laminates failed with extensive delamination.

The different damage modes of the two laminate types led to different behaviour between the specimens with regards to the ultimate stress. For the single ply specimens, the initiation of damage was seen as only matrix damage, and the specimen failed in net tension. For this failure, the stress at damage initiation (from observation) was 61% of the stress at maximum load. For the four ply specimens, the occurrence of delamination led to a delay between the onset of damage and the maximum load. As such, the stress at damage initiation was only 29% of the stress at maximum load. This difference can be seen as a large increase in the region between σ_{obs} and σ_{max} in Fig. 3. The extent of the increase is such that the maximum stress for the four ply specimens was higher than the single ply specimens, despite damage initiation occurring at lower strain.

The increase in maximum stress of the four ply specimens was attributed to the different energy-absorbing mechanisms of the two failure modes. The increased prevalence of delamination in the four ply specimens would have required more energy, and higher loads. This was due to the damage process in the four ply specimens being more diffuse, with cracks branching between layers and at multiple layers simultaneously. This avoided high stress concentrations triggering early failure. In contrast, with only minor matrix cracking in the single ply specimens, the hole edge continued to be highly loaded, and fibre failure initiated at an earlier stage.

3.3 1.0” hole (OH-05) Specimens

For the 1.0” hole specimens, the results and conclusions were very similar to the 0.5” hole specimens. The initiation of damage was observed to occur at around 60% of the damage initiation strain in the un-notched specimens. This was a slight increase from the 0.5” hole specimens, where the strain at damage initiation was around 48% of the un-notched value. In contrast, the stress at damage initiation was more or less constant with increasing hole size, with stresses around 250 MPa and 150 MPa seen to initiate damage in the single and four ply specimens for both hole sizes.

With regards to maximum load, specimen characteristics and damage mode, the same behaviour was seen as described for the 0.5” hole specimens. For the single ply laminates, although the damage initiation was clearly noticeable, there was only mild non-linearity. As such, the 5% NL strain values corresponded to the maximum load. As with the 0.5” specimens, the 1.0” single ply specimens showed only monotonically increasing load and strain values to ultimate load, which is indicative of only mild matrix cracking.

For the four ply specimens, the behaviour of the 1.0” hole specimens was very similar to that for the 0.5” hole specimens previously described. The initiation of damage was seen to trigger several occurrences of delamination growth (two to three were common), which was evidenced by step changes in the load and strain data. The failure mode of the specimen following ultimate load was delamination, which acted to delay the maximum load. The difference between damage initiation and maximum stress was therefore higher, and the maximum stress of the four ply laminates was higher than that for the single ply laminates. Comparing to the 0.5” hole specimens, the maximum stress values of the 1.0” hole specimens were slightly reduced, though the damage initiation values were very close as previously discussed.

For the 1.0” hole specimens of both laminates, evidence of grip slippage was seen at loads in excess of around 90 kN. This was detected in a significant change in slope (~50%) in the load-displacement data from the test machine, and occurred for 10 out of 12 1.0” hole specimens. Although the test machine crosshead displacement is unreliable as a measure of specimen displacement due to the compliance in the machine, a large change in slope is nonetheless evidence of a change in specimen behaviour. There were no tabs or attachments as part of the gripping arrangement, with only sandpaper being used between the specimen in the grips. Despite this, the load-strain results for all specimens did not show any change in character or additional non-linearity that could be attributed to grip slippage.

3.4 Optical Full-Field Strain Data

Examples of the optical strain data are given in Fig. 6, which shows the strain of the surface 45° ply in the *x* and *y* directions at two different stress levels after damage initiation. From these, the asymmetric nature of the stresses due to the occurrence of damage at the hole edge can be seen. Although a detailed study of the strain data has not yet been conducted, the results showed excellent agreement with strain gauge data, as shown in Fig. 7, and further illustrated damage development and strain non-linearity.

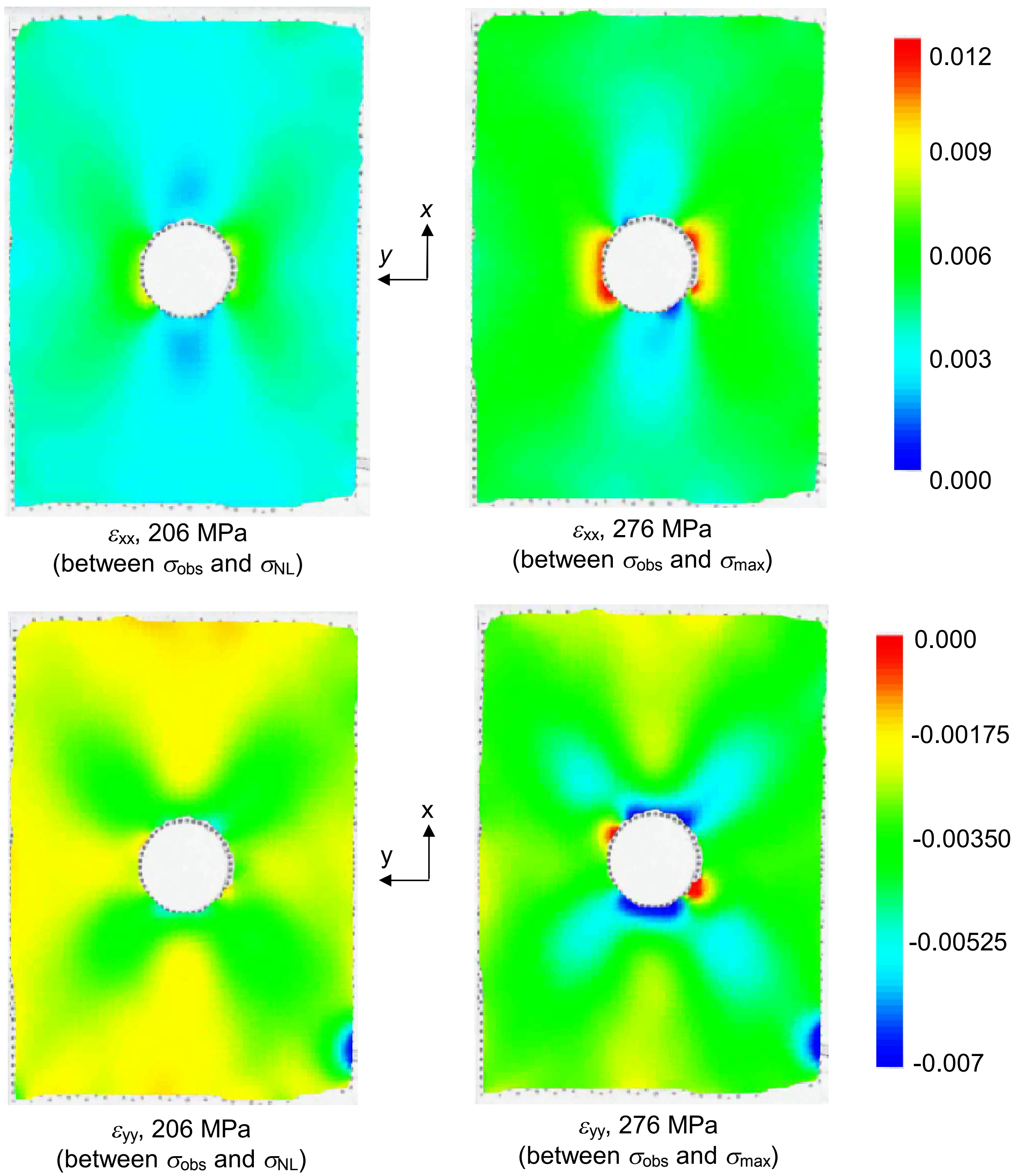

Fig. 6. Strain sequences (four ply, 1.0" hole, specimen #6)

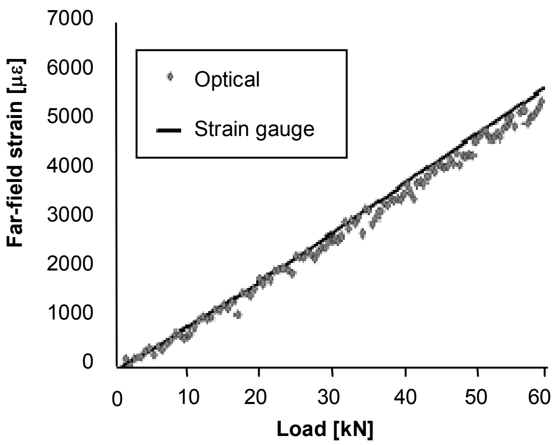

Fig. 7. Comparison of far-field strain data from optical and strain gauge measurement

3.5 Length Scale Effects

There were two changes of length scale in the experimental testing conducted: change of ply thickness through the use of the single ply and four ply laminates; change in specimen geometry though scaling the in-plane dimensions with the hole diameter.

With regards to the change in ply thickness, the results demonstrated that the effect of increasing the ply thickness was reduced ply strength. This was seen as lower ultimate strength and strain, as well as the non-linearity associated with damage occurring at lower strain levels.

The change in ply thickness also resulted in a change of failure mode, and a fundamental change in the specimen behaviour at higher loads. Matrix cracking at the hole edge for the thicker ply specimens was shown to lead to the occurrence of delamination between plies. This led to a more progressive and diffuse damage progression, which increased the ultimate strength. These results demonstrate the link between matrix cracking and delamination, and the energy-absorbing characteristics of delamination growth.

For the change in specimen geometry, the results showed that doubling the in-plane dimensions led to a slight decrease in the ultimate stress, an increase in the strain at damage initiation, and no change in the stress at damage initiation. This demonstrates the complexity of the scale effect phenomena, which are related to the scale of the notch relative to the specimen dimensions, and also to the ply thickness. The results in this set of experimental testing suggest that the ultimate strength of the notched specimens is related to the notch size to a small degree. On the other hand, the results suggest that the initiation of damage, in the form of matrix cracking, is related more to the ply thickness, as opposed to the specimen or notch dimensions. Further work is required in order to verify that these conclusions remain valid across different specimen configurations.

4 Discussion

One aspect that was important in contributing to both the behaviour of the specimens and the scatter in the experimental results was the occurrence of damage in the specimens during manufacture. Following manufacture, it was noticed that there was backface delamination and ply splitting at the hole edge for some specimens. The size of this damage was of the order of $0.1d$, where d is the diameter of the hole. It is thought that for some specimens this manufacturing damage acted as the starting point for crack growth, although damage propagation from other locations was seen for many specimens.

The results of this investigation are of critical importance for the development of predictive tools for composite laminate failure, where currently the interaction between length scales is not taken into account. This results in the need for expensive experimental testing at all the length scales from the coupon level to the structural level, as part of the current industry standard of the Building Block Approach (BBA). The results presented in this work are part of a broader collaborative research project that aims to develop an alternative to the BBA using an energy-based multi-axial material characterisation methodology for composite materials, which is capable of incorporating length scale effects. Further detail on this approach can be found in separate publications, which cover the development of multi-axial testing method [6], specimen design [7], and initial development of an analysis approach [1].

5 Conclusion

An experimental investigation was conducted to study the effect of notch size and length scale on the damage performance of carbon fibre-reinforced composite specimens. Open hole tension specimens were tested at two hole sizes and two ply thicknesses, and compared to results for an un-notched laminate. The results showed that:

- Increasing the ply thickness by a factor of 4 reduced the ultimate strength of the un-notched specimen by 16%.
- The introduction of the hole caused damage initiation at 48% of the un-notched damage initiation strain for both ply thicknesses.
- The thinner ply laminate showed strain non-linearity associated with matrix cracking at the hole edge at around 50% of the ultimate load. The damage mode after ultimate load was tension failure with fibre fracture dominant spreading perpendicular from the hole edge.
- The thicker ply laminate showed strain non-linearity associated with matrix cracking at the hole edge leading to extensive delamination prior to ultimate load. The development of delamination absorbed a lot of energy, so that despite the initiation of damage occurring at lower loads, the average ultimate load was higher than the thinner ply laminate.
- Increasing the hole size and in-plane dimensions slightly reduced the maximum stress, whilst initiation of damage was more suitably linked with the ply thickness than with the in-plane dimensions.
- The analysis of full-field strain data provides a wealth of data on the non-linearity of the strain field and the development of damage.

The output of the testing provides key insights into damage behaviour and scale effects of composite materials, and is also critical for the development and validation of predictive tools for damage analysis.

References

[1] Litchfield AJ, Thomson RS, Orifici AC. Analysis of damage development in CFRP notched coupons with energy-based multi-axial failure data. *27th Congress of the International Council of the Aeronautical Sciences*, Nice, France, 19-24 September 2010.

[2] Andrianopoulos NP and Iliopoulos AP. Strain measurements by a hybrid experimental-numerical method using a mesh-free field function. *Honorary Volume for Professor P. S. Theocaris*, Armenian Academy of Sciences, pp. 31-41, 2005.

[3] Andrianopoulos NP. Full-field displacement measurement of a speckle grid by using a mesh-free deformation function. *Strain*, Vol. 42, pp. 265-271, 2006.

[4] Andrianopoulos NP and Iliopoulos AP. Displacements measurement in irregularly bounded plates using mesh free methods. *16th European Conference of Fracture*, Alexandroupolis, Greece, July 3-7, 2006.

[5] Iliopoulos AP. *Digital Image Processing on Experimental Mechanics and Applications on Metallic Sheets*. PhD Thesis, National Technical University of Athens press, Athens, (In Greek), 2007.

[6] Michopoulos JG, Hermanson JC and Furukawa T. Towards the robotic characterization of the constitutive response of composite materials. *Composite Structures*, Vol. 86, pp. 154-164, 2008.

[7] Orifici AC, Michopouls JG, Lagace PA and Herszberg I. Composite material specimen design for validation of an energy-based multi-axial failure methodology. *4th International Conference on Composite Testing and Model Identification*, Dayton, Ohio, USA, 20-22 October, 2008.

Acknowledgments

This research is part of the Research Program of the CRC-ACS, and is partly supported by the US Office of Naval Research under NICOP grant N00014-07-1-0514. The authors gratefully acknowledge the assistance in experimental testing of Mark McVilley and Alex Zislin of CRC-ACS, and Vanessa Pickerd of Monash University, in addition to Dr Athanasios Iliopoulos of the U.S. Naval Research Laboratory for processing the optical strain data.

Copyright Statement